Increasing Efficiency of a Wireless Energy Transfer System by Spatial Translational Transformation

Shichao Li, Fei Sun, Di An, and Sailing He, *Fellow, IEEE*

***Abstract*—A magnetic translational projector (MTP) designed by transformation optics is applied to improve energy transfer efficiency in a wireless power transfer (WPT) system. Our numerical simulation results show the MTP can greatly enhance energy transfer efficiency (e.g., nearly two orders, compared to the case without our MTP) in the WPT system, which is much larger than that of a previous method (i.e., using magnetic super-lens). A 3-D reduced MTP composed of layered isotropic magnetic materials is designed, whose performance is verified by our 3-D numerical simulation in 10 MHz. The influence of loss in metamaterial on the performance of the proposed MTP is also studied, which shows that the MTP can still enhance energy transfer efficiency when loss exists. Further simulation is also carried out to show that the function of the MTP is not sensitive to large perturbation. Finally, detailed experimental suggestion for implementing the simplified MTP, which is composed of layered medium is given and then verified by our numerical simulation.**

***Index Terms*—Magnetic device, metamaterial, transformation optics, wireless energy transfer.**

I. Introduction

EFFORT to transfer energy wirelessly was made in an early human history, which began from Nikola Tesla [1]. Wireless energy transmission technology has many important applications, e.g., charging biomedical implants [2], unmanned vehicles [3], etc. One important challenge in this field is to increase energy transfer efficiency.

Manuscript received November 6, 2016; revised February 10, 2017 and April 10, 2017; accepted May 2, 2017. Date of publication May 11, 2017; date of current version January 3, 2018. This work was supported in part by the National Natural Science Foundation of China (91233208and 60990322), in part by the National Natural Science Foundation of China for Young Scholars (11604292), in part by the National High Technology Research and Development Program (863 Program) of China (2012AA030402), in part by the fundamental research funds for the central universities (2017FZA5001), in part by the Program of Zhejiang Leading Team of Science and Technology Innovation, the Postdoctoral Science Foundation of China (2013M541774), in part by the Preferred Postdoctoral Research Project Funded by Zhejiang Province (BSH1301016), in part by the Swedish VR Grant (#621-2011-4620) and AOARD. Recommended for publication by Associate Editor C.-K. Tse. *(Corresponding Author: Fei Sun.)*

S. Li, F. Sun, and D. An are with the Center for Optical and Electromagnetic Research (COER), College of Optical Science and Engineering, Zhejiang University, Hangzhou 310058, China (e-mail: nicholas_lee@zju.edu.cn; sunfei@zju.edu.cn; 303091410@qq.com).

S. He is the Center for Optical and Electromagnetic Research (COER), College of Optical Science and Engineering, Zhejiang University, Hangzhou 310058, China, and is also with Department of Electromagnetic Engineering, School of Electrical Engineering, Royal Institute of Technology (KTH) S-100 44 Stockholm, Sweden (e-mail: sailing@kth.se).

Color versions of one or more of the figures in this paper are available online at http://ieeexplore.ieee.org.

Digital Object Identifier 10.1109/TPEL.2017.2703591

To avoid system complexities and the possible health risk of far-field radiative power transfer, quasi-static (low-frequency) electromagnetic (EM) field is more suitable for mid-range wireless power transfer (WPT) system [4]. Using inductive coupling between two coils is one way to achieve energy transfer. However, the energy transferred is limited in a short range as magnetic flux decays rapidly with increasing distance. In 2007, the strongly coupled magnetic resonance scheme [5] was proposed to increase the coupling efficiency of two coils in a WPT system, and was later further explored and developed [6]. This is a method that changes energy transfer scheme in a WPT system. Adding other devices in a WPT system is another way to improve energy transfer efficiency. Magnetic superlens with negative permeability was theoretically shown to be helpful in improving energy transfer efficiency [7]. Then, this method was experimentally validated with the help of metamaterials [8]–[10].

Transformation optics (TO) serves as a theoretical tool for designing these devices. Since it was proposed in 2006 [11], it has helped scientists controlling EM field in a pre-designed manner. From the perspective of TO, a superlens can be designed by a space folding transformation [12]. Apart from superlens, other magnetic devices were also designed using TO. For instance, magnetic concentrator based on space compression transformation [13] was theoretically proposed to enhance energy transfer efficiency. Later with the help of metamaterials, such magnetic concentrator was experimentally demonstrated [14].

In this paper, we use the magnetic translational projector (MTP) based on the spatial translational transformation [15] to improve energy transfer efficiency in WPT systems. Such MTP can greatly enhance energy transfer efficiency in WPT systems. We have designed a 3-D reduced structure composed of layered isotropic magnetic materials to realize the proposed MTP in 10 MHz, whose performance is verified by our 3-D numerical simulation based on finite element method (FEM). We also numerically study the influence of loss and perturbation on the performance of the proposed MTP. Compared with the previous method, the proposed method in this paper can achieve a better enhancement of energy transfer efficiency in WPT systems.

In Section II, we briefly explain TO and use it to design the MTP theoretically. We also give the physical explanation about how to improve the energy transfer efficiency by our MTP. In Section III, we elaborate on how we establish our numerical model, and carry out numerical studies on the performance of our MTP. In Section IV, we compare the performance of our MTP with traditional magnetic superlens, and propose the realization method of our MTP based on the effective medium theory and metamaterial.

II. Theoretical Background

TO is a new and powerful theoretical tool to design novel EM devices such as invisibility cloaks [11], magnetic concentrators [13] ,[14], and optical wormholes [16]. We have two spaces in TO: one is the reference space (i.e., a virtual space), where Maxwell's equations can be described as $\nabla \times \boldsymbol{E} + i\omega\mu\boldsymbol{H} = 0$, $\nabla \times \boldsymbol{H} - i\omega\varepsilon\boldsymbol{E} = \boldsymbol{J}$, $\nabla \bullet \boldsymbol{B} = 0$, $\nabla \bullet \boldsymbol{D} = \rho$. The other is the real space, where Maxwell's equations can be described as $\nabla \times \boldsymbol{E}' + i\omega\mu'\boldsymbol{H}' = 0$, $\nabla \times \boldsymbol{H}' - i\omega\varepsilon'\boldsymbol{E}' = \boldsymbol{J}'$, $\nabla \bullet \boldsymbol{B}' = 0$, $\nabla \bullet \boldsymbol{D}' = \rho'$. We use the coordinate transformation [e.g., $(x, y, z) \rightarrow (x', y', z')$] to establish relationship of quantities between the two spaces. To keep the form-invariance of Maxwell's equations in the two spaces, the EM medium (i.e., relative permittivity and permeability) in two spaces should satisfy the following relations [11]: $\varepsilon'^{i'j'} = |\det(\Lambda_i^{i'})|^{-1}\Lambda_i^{i'}\Lambda_j^{j'}\varepsilon^{ij}$, $\mu'^{i'j'} = |\det(\Lambda_i^{i'})|^{-1}\Lambda_i^{i'}\Lambda_j^{j'}\mu^{ij}$ $(i, j = 1, 2, 3)$. Here, $\Lambda_j^{i'}$ is the Jacobian transformation matrix between the real space and the reference space (i.e., $\Lambda_1^{1'} = \partial x'/\partial x$, $\Lambda_2^{2'} = \partial y'/\partial y$, $\Lambda_3^{3'} = \partial z'/\partial z$). It means that we can use the coordinate transformation to design a medium with a predesigned function with the help of TO. In many designs, people often assume the reference space is free space (i.e., $\varepsilon = \mu = 1$). The medium designed by TO is often complicated (i.e., anisotropic and inhomogeneous), which can still be implemented by metamaterial [17], [18].

To achieve a longer energy transfer distance or higher energy transfer efficiency in a WPT system, we can use a device that can transfer more magnetic energy from the source coil to the receiving coil. In other words, this device should redirect the EM field generated by the source coil to a further distance. In the perspective of optics, a lens usually can achieve such a function, since it can refocus the EM field of the source. A magnetic superlens is an example [19]. Our aim is to design a special lens/shell that can project/shift the EM source (e.g., the source coil) by a predesigned distance *d* to another spatial position outside the lens/shell. It means that if an EM source is set in such a shell (i.e., our MTP), the EM field outside the shell is the same as the field produced by, an imaginary EM source located at the position shifted by a distance *d* from its real position.

A. Transformation Relationship

The MTP shell (purple region) shown in Fig. 1(a) can achieve such a function. Here, we use quantities with and without primes to indicate the quantities in the real space and reference space, respectively, which consists with previous definition in TO [15]. The material of the white and red regions is air, due to the identity transformation (i.e., $x' = x$, $y' = y$, $z' = z$) and the spatial translational transformation along x' direction (i.e., $x' = x - d$, $y' = y$, $z' = z$), respectively [15]. The purple region where our MTP lies is filled with special medium, in which the

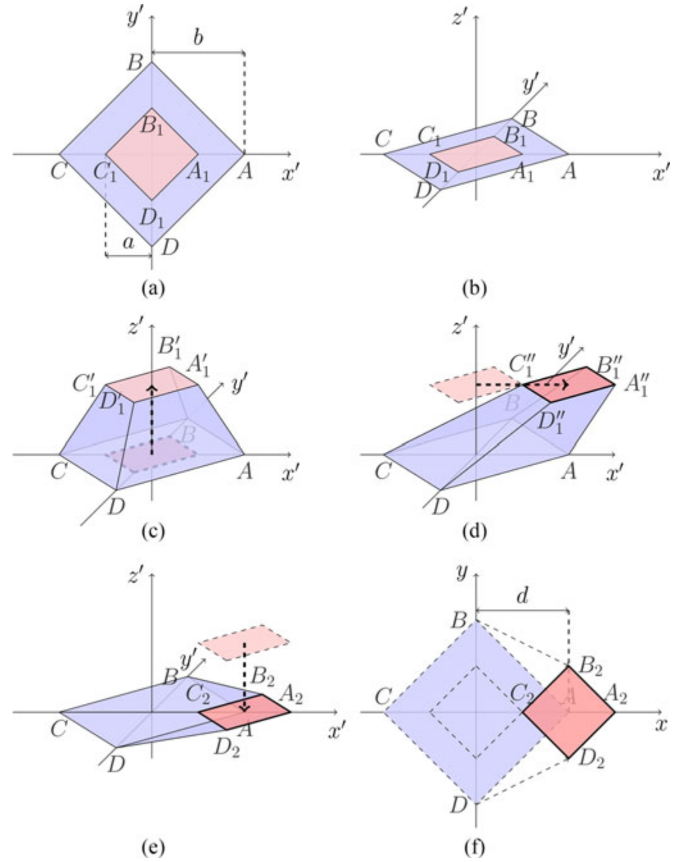

Fig. 1. (a) Proposed MTP in the real space. (b)–(f) show the whole process of the spatial translational transformation from the real space to the reference space.

coordinate transformation is given by

$$x' = \begin{cases} -(b-a)x/(d-b+a) - dy/(d-b+a) \\ +db/(d-b+a), \\ \text{for region in the first quadrant} \\ (b-a)x/(d+b-a) + dy/(d-b+a) \\ -db/(d+b-a), \\ \text{for region in the second quadrant} \\ (b-a)x/(d+b-a) - dy/(d+b-a) \\ -db/(d+b-a), \\ \text{for region in the third quadrant} \\ -(b-a)x/(d-b+a) + dy/(d-b+a) \\ +db/(d-b+a), \\ \text{for region in the forth quadrant} \end{cases}$$

$$y' = y, \quad z' = z \tag{1}$$

where *a* and *b* are geometrical parameters of the MTP [see Fig. 1(a)]. *d* is the translational distance, which means how far the imaginary source is away from the real source.

B. Explaining the Coordinate Transformation

The coordinate transformation relationship of the proposed MTP [described by (1)] can be understood in Fig. 1. From Fig. 1(b) to (f), the 2-D spatial translational transformation carried out for the MTP [purple regions in Fig. 1(a)] from the real space to the reference space is given vividly: the red square domain $A_1B_1C_1D_1$, where the source coil is located, is stretched outside of the $x' - y'$ plane along z' direction [see Fig. 1(b) and (c)]. This $A_1'B_1'C_1'D_1'$ region is then shifted by a predesigned distance *d* along x' direction from Fig. 1(c) to (d). Finally, we press down $A_1''B_1''C_1''D_1''$ to the $x' - y'$ plane and obtain a spatially translated new square region $A_2B_2C_2D_2$, where we want the imaginary EM source to be.

From the perspective of TO, any magnetic source inside the region $A_1B_1C_1D_1$ enclosed by the MTP (i.e., the anisotropic medium given by (2) in the purple region between $A_1B_1C_1D_1$ and *ABCD*) will be shifted to the region $A_2B_2C_2D_2$ outside the MTP. This means if a source coil is placed inside the MTP, the magnetic field inside the MTP produced by the source coil can be shifted rightward to a predesigned image position in free space outside the MTP. The final magnetic field is like that generated by an imaginary source coil placed at the predesigned position in free space without the MTP. Hence, after covering the source coil with the MTP, an "image" coil is created at the predesigned position. Assuming there is a receiving coil located at the predesigned position, the "image" of the source coil will overlap the receiving coil, so that the energy transfer efficiency can be greatly enhanced.

C. Intrinsic Parameter Calculation

According to the theory of TO, the required relative permeability and permittivity in the purple region in Fig. 1(a) is determined by the transformation relationship. Calculation in [15] shows that the device used to achieve the aforesaid function is a uniform anisotropic medium with the following relative permittivity and permeability:

$$\mu' = \varepsilon' = \begin{bmatrix} \frac{(P^2+Q^2)}{P} & \frac{Q}{P} & 0 \\ \frac{Q}{P} & \frac{1}{P} & 0 \\ 0 & 0 & \frac{1}{P} \end{bmatrix} \tag{2}$$

where $P = -\text{sign}(x')\Delta/(d - \text{sign}(x')\Delta)$, $Q = -\text{sign}(x')\text{sign}(y')d/(d - \text{sign}(x')\Delta)$, and $\Delta = b - a$. $\text{sign}(x') = 1$ if $x' > 0$, and equals - 1 otherwise. Note that we have assumed the medium is air (i.e., the relative permeability and permittivity are 1) in the reference space in the above calculation.

As a low-frequency EM source (e.g., $f = 10$ MHz) is adopted for the WPT system, quasi-static approximation indicates that the electric field and magnetic field are decoupled [8]. This is the reason why we only need to consider the relative permeability of the device. Therefore, we set the relative permittivity in our device as

$$\varepsilon' = 1. \tag{3}$$

Hence, the optical translational projector in [15] becomes our MTP. To get a 3-D MTP, we can extend the 2-D MTP in z' direction, whose relative permeability and permittivity are given by (2) and (3), respectively.

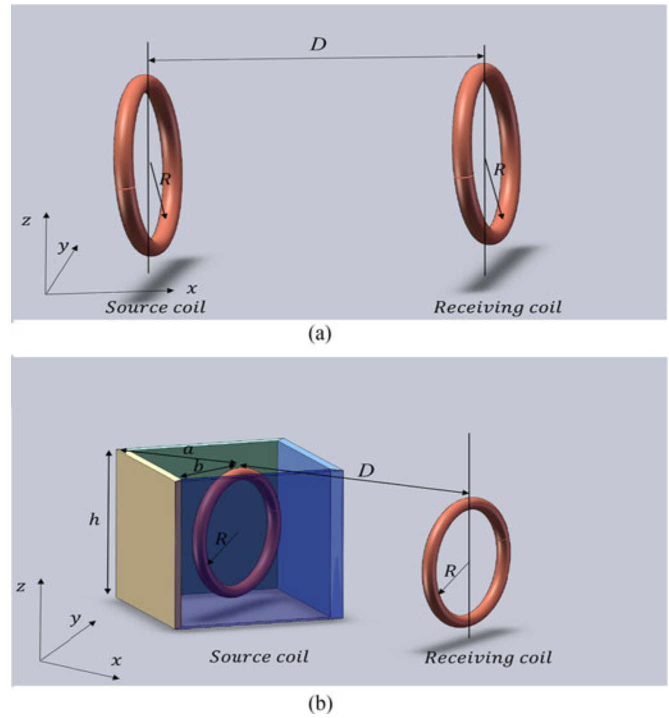

Fig. 2. (a) Diagram of a simplified WPT system. (b) Adding MTP in the WPT system. *R* is the radius of the copper coil. *D* is the distance between the two coils. *a*, *b* are outer and inner sizes of the MTP, respectively. In this model, $a = 0.7$ m, b = 0.8 mD = 1 m, h = 1 m, and $R = 0.5$ m.

III. Modeling Results

A. Model Setup

Two copper circular antennas are utilized to build a simplified WPT system [see Fig. 2(a)]. One coil called source coil carries externally injected current and excites EM field, which leads to induction current on the other one. The coil in which induced current flows is designated as the receiving coil.

We set a constant external current density excitation along the tangential direction in the source coil. Specifically, the radial current component J_r is zero, whereas the tangential current J_θ is set as a constant (1 A/m^2). Energy is transferred from the source coil to the receiving coil via magnetic coupling. Fig. 2(b) shows that the designed MTP is added around the source coil to improve the energy transfer efficiency. The working frequency in our simulation is chosen as 10 MHz in this study, which has the same order as those used in former studies [20]. A FEM solver (COMSOL Multiphysics) is used to solve wave equation. In all simulations, we use a single-turn circular coil in order to reduce computation time, whereas in realistic situations these coils may be more complex. However, our MTP should still give a good energy transfer efficiency enhancement in realistic situations. That is because our MTP can project the magnetic source inside it to further region, no matter what the shape of magnetic source is.

B. EM Field Modification

The norm of the magnetic field intensity produced by the source coil, whose distribution resembles that of a magnetic

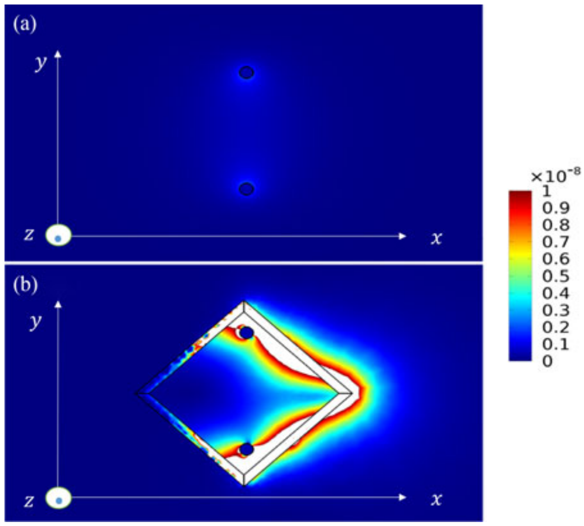

Fig. 3. Two-dimensional distribution of the norm of magnetic field: (a) without the MTP, and (b) with the MTP ($d = 0.9$ m, a $= 0.7$ m, b $= 0.8$ m, and $R = 0.5$ m, d is the translational distance of the MTP). Here, white regions mean the field intensity is beyond the maxima of the color bar.

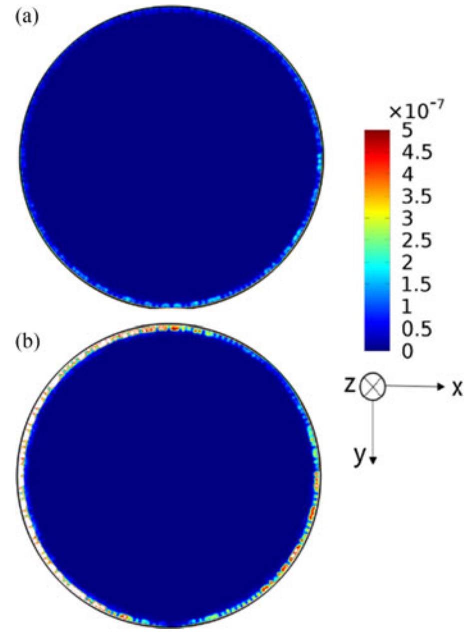

Fig. 4. Two-dimensional distribution of the amplitude of surface current density on the cross section of the receiving coil: (a) without the MTP and (b) with the MTP. The geometrical parameters of the MTP and the two coils are the same as Fig. 3, and they remain unchanged in Figs. 5–7. The white regions mean the field intensity is beyond the maxima of the color bar.

dipole, is shown in Fig. 3(a). When the source coil is covered with the MTP, the magnetic field is obviously altered [see Fig. 3(b)]. A much stronger magnetic field is observed on the right side of the coil, which means the MTP can help the source coil transfer more energy to its right side. This effect suggests better energy transfer efficiency in larger distance.

C. Induction Current Enhancement

With the help of the MTP, more magnetic flux is transferred to the receiving coil, which results in a larger inductive current inside the coil, and hence a higher energy transfer efficiency. The surface current density distributions on the cross section of the receiving coil without and with the MTP are plotted in Fig. 4(a) and (b), respectively. This intersection plane bisections the source coil, and lies in the *x*-*y* plane. Evidently, the inductive current on the receiving coil is greatly enhanced by the MTP. The inductive current is mainly located on the edge of the coil due to skin effect.

Surface integration of current density on the cross section of the two coils is calculated. The ratio is plotted in Fig. 5, in a logarithmic manner, where I is the integration of current density on the receiving coil, and I_s is the integration on the source coil. I_s is a constant of 4.64×10^{-7} A, which is the current we inject into this coil. We can see that our MTP can greatly increase the current inside the receiving coil. As distance between these two coils increases, the inductive current on the receiving coil decreases. However, the inductive current on the receiving coil is always enhanced by introducing our MTP, compared with the case without the MTP.

D. Power Enhancement

To make a quantitative comparison with other methods, we define the enhancement factor of the energy transfer

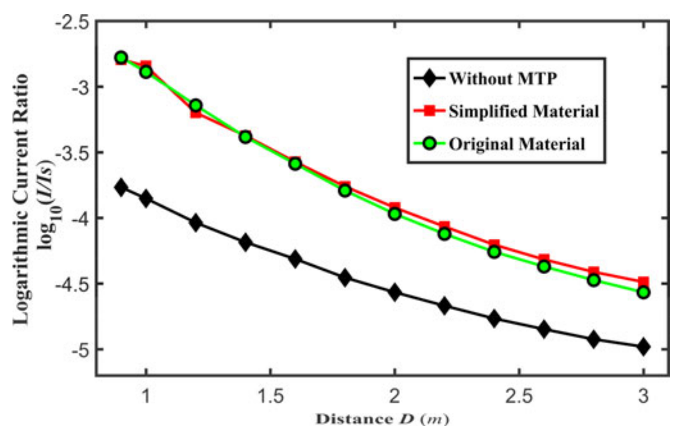

Fig. 5. Ratio of surface current density integration as the distance D between the two coils changes. I is the current density integration on the cross section of the receiving coil, while I_s is that of the source coil. The z-component of the permeability for the simplified material is reduced to 1.

efficiency by

$$A = \frac{P_{\mathrm{MTP}}}{P_0} \tag{4}$$

where P_{MTP} and P_0 are Joule heat produced on the receiving coil with and without the MTP, respectively. This definition consists with previous studies, in which power dissipated on the load is used to measure the power harvested by the receiving coil [4], [8], [14].

To reduce the complexity for realizing the proposed MTP, we make a simplification on the material requirement and propose a simplified MTP. In the simplified version, the negative permeability in the z direction of the MTP is set as 1, which

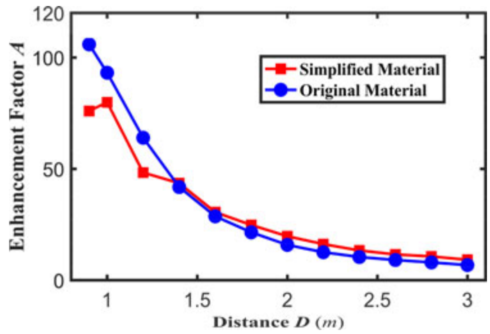

Fig. 6. Enhancement factor *A* of the energy transfer efficiency defined by (4) versus distance *D* between two coils.

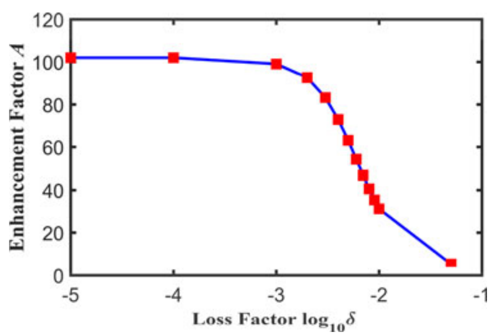

Fig. 7. Relation between enhancement factor *A* and loss factor $log_{10}\delta$.

greatly facilitates experimental implementation. The numerical simulation results in Figs. 5 and 6 show such a reduced MTP can also give a good coupling enhancement between two coils.

Metamaterials are required to realize the proposed MTP, as some regions of the MTP (i.e., in the first and forth quadrants of our MTP) need negative permeability due to the spatial folding transformation. The loss of resonate metamaterials to achieve such a negative permeability will affect the performance of our MTP. In realistic resonate negative permeability metamaterial structures, loss can be described by an imaginary part of permeability. Loss varies with different structures and designs, but imaginary part near or smaller than 1 is common in present low-loss metamaterials [9], [21], and can even approach zero [22].

To know how loss affects the performance of our MTP, we carry out numerical simulation in the WPT system, when a small imaginary part $i\delta$ (i.e., loss) is added on the required negative permeability of the MTP (see Fig. 7). Although the enhancement factor *A* defined by (4) decreases as the loss δ in the metamaterial increases, our MTP can still give a good energy transfer efficiency enhancement (i.e., $A >> 1$). In our simulation, loss is added on the whole structure of our MTP. However, loss usually only exists in the metal regions of metamaterial in realistic situation. These metal regions usually are very thin (i.e., the imaginary part we added in our simulation can only exaggerate loss influence on our MTP).

E. Position and Orientation Sensitivity

In realistic situation, the position and orientation of the MTP relative to the source coil may influence its function. To study this effect, we plot the magnetic field distribution (see Fig. 8) when the location and orientation of inner coil changes (the position and the orientation of the MTP keep unchanged). Since the coil acts like a magnetic dipole, more energy is transferred along the central axis of the coil. Thus, when the coil is rotated, the magnetic field on the right side of the MTP is weaker than when the central axis of the coil aligns with *x*-axis. However, we can see that even if a severe perturbation (rotation or movement) is present, our MTP can still direct a large amount of energy to the right side of the MTP.

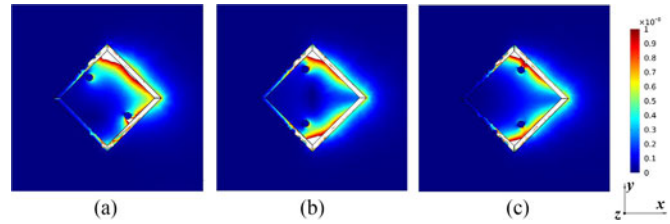

Fig. 8. Two-dimensional distribution of the norm of magnetic field when perturbation is considered. (a) Coil is rotated 45° around the center of the MTP. (b) and (c) coil is shifted 0.1 m along –*x*- and *x*-axes, respectively.

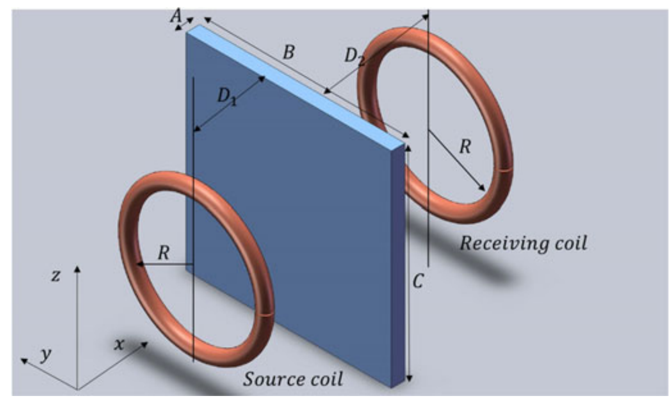

Fig. 9. Diagram of a WTP system using a magnetic super-lens (i.e., the blue slab has $\mu_r = -1$).

IV. Performance Comparison and Realization Proposal

A. Comparison With Former Method

A magnetic superlens with negative permeability (see Fig. 9) is a traditional way to enhance energy transfer efficiency in WPT systems. It can be designed by a 1-D spatial folding transformation along *x* direction [12]. This leads to an infinitely large size of superlens in both *y* and *z* directions (*B* and *C* in Fig. 9 should be infinitely long). A practical 3-D super-lens with a finite length in both *y* and *z* directions (i.e., truncated in two directions) will greatly influence its performance. Our MTP utilizes 2-D folding transformation, thus it can achieve the full function in a 2-D plane with a finite size. For a 3-D MTP, it should be infinitely long in *z* direction (*h* in Fig. 2(b) should be infinitely large). Thus, for a 3-D practical MTP we approximate in *z* direction, which also limit the performance of our MTP. However, for a 3-D practical structure, our MTP makes truncation in only one direction whereas the super-lens makes truncation in two directions (e.g., both *y* and *z* directions). This

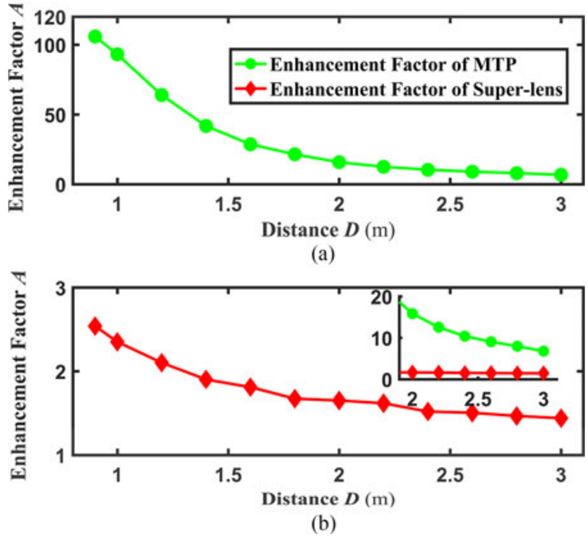

Fig. 10. Enhancement factor A in a WTP system using (a) 3-D MTP with height $h = 1$ m (other parameters are the same as those for Fig. 2), and (b) traditional superlens with $A = 0.1$ m, and $B = C = 1.5$ m in Fig. 8. The zoom-in inset shows the comparison when the distance D exceeds 2 m.

indicates our MTP should give a much better performance than a superlens.

To make a comparison between our MTP and a superlens, we choose $D_1 = D/2 = 0.45$ m in Figs. 2(b) and 9. The theoretical image of the superlens will be 0.9 m away from the source coil, which coincides with the image distance of our MTP since $d = 0.9$ m. To make a fair comparison, the thickness and height of the superlens and MTP are chosen to be the same. The numerical simulation shows our MTP can achieve a much higher efficiency than superlens (see Fig. 10).

B. Implementation Proposal

We can use layered isotropic media to realize the required homogenous anisotropic permeability, based on the effective medium theory [23]. To realize the proposed MTP, we need first to find the direction of the principal axes and principal values of the required anisotropic permeability in (2). The symmetric permeability tensor in (2) can be diagonalized by a coordinate rotation around the z direction, leading to three principle values: $\lambda_{1,2} = (\alpha + \gamma \pm \sqrt{(\alpha - \gamma)^2 + 4\beta^2})/2$ and $\lambda_3 = \gamma$, where $\alpha = (P^2 + Q^2)/P$, $\beta = Q/P$, and $\gamma = 1/P$. We denote the portion of our MTP in quadrants I– IV as regions 1– 4. Due to symmetry, regions 1 and 4 have the same principle values after diagonalizing, so do regions 2 and 3.

In the case of simplified MTP, to realize one of the regions aforementioned, we only need to arrange two isotropic media periodically in the x-y plane, since variety in z direction is omitted. In addition, taking advantage of symmetry to achieve our MTP, the total number of materials with different permeability can be as less as 4, and only two types of these materials need to have negative permeability.

Fig. 11 shows one possible way to implement the proposed simplified MTP. The required anisotropic permeability is

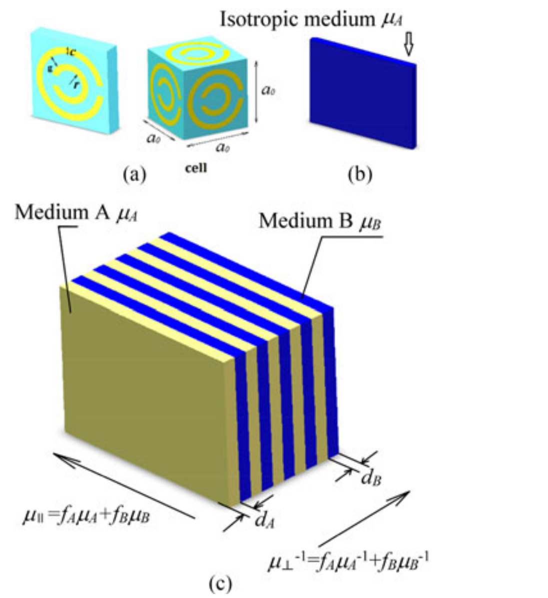

Fig. 11. (a) Diagram of traditional SRR structure (left), and a 3-D cell with three SRRs on cell surface to achieve a negative permeability. If all SRRs have the same geometrical parameters, the 3-D periodic structure can be treated as an isotropic medium. (b) Diagram of an effective medium composed of metamaterial cells in (a). (c) Two isotropic media with different permeabilities to realize the required anisotropic permeability according to the effective medium theory.

realized by layered material with isotropic permeability based on the effective medium theory [23], as shown in Fig. 11(c). If the wavelength of the incident EM wave is much larger than the size of each layer, the effective relative permeability of the whole structure can be described by [23]

$$\begin{cases} \mu_\perp^{-1} = f_A\mu_A^{-1} + f_B\mu_B^{-1} \\ \mu_\parallel = f_A\mu_A + f_B\mu_B \end{cases} \tag{5}$$

where $\mu_{\rm A}$ and $\mu_{\rm B}$ are relative permeability of two layered materials A and B, respectively, in Fig. 11(c). Subprime $||$ and $\perp$ indicate the direction parallel and perpendicular to the interface between medium A and medium B, respectively. $f_{\rm A} = d_{\rm A}/(d_{\rm A} + d_{\rm B})$ and $f_{\rm B} = d_{\rm A}/(d_{\rm A} + d_{\rm B})$ are filling factors of medium A and medium B, respectively. Based on the effective medium theory in (5), we can use two isotropic homogeneous magnetic materials to achieve the required anisotropic permeability in our MTP. In regions 1 and 4 [see (1) and (2)] negative permeability is needed. There have been numerous kinds of metamaterial structures used to achieve negative relative permeability [9], [10], [24], [25]. Actually, we can realize a very wide range of permeability (e.g., negative permeability, extremely large permeability, and permeability near zero) by tuning geometrical parameters of these kinds of metamaterial structure at required frequency.

As an example, in regions 1 and 4, we can use split-ring resonators (SRRs) to achieve the required negative permeability [see Fig. 11(a)] [25]. Sticking three identical SRRs on a cubic cell can form a 3-D periodic medium, which has isotropic relative permeability that can be described as $\mu_{\rm eff} = 1 - (\frac{\pi r^2}{a_0})/(1 + \frac{2a_0\sigma_1 i}{\omega r\mu_0} - \frac{3a_0c_0^2}{\pi\omega^2\ln(\frac{2cr^3}{g})})$ [25]. σ_1 is the

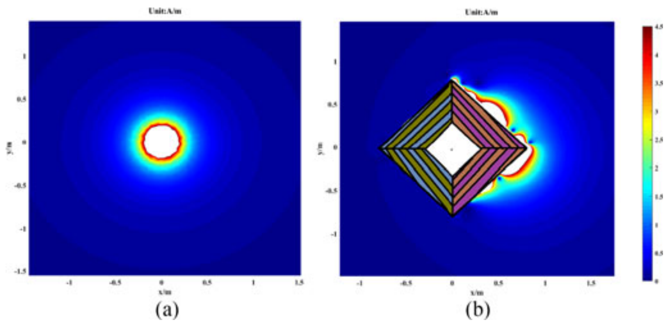

Fig. 12. Magnetic field norm distribution of (a) point magnetic dipole without MTP and (b) point magnetic dipole covered by the MTP composed of layered isotropic medium. Note the number of layers is exaggerated to show the method clearly, and in fact 15 layers are adopted in each quadrant of the MTP. Every kind of color of the layers indicates one type of material (i.e., the designed isotropic relative permeability of the orange, purple, blue, and green regions are -36.36, -0.0275, 36.26, and 0.0276, respectively). The filling factors are designated as 0.5 for each double-layered region in each quadrant. All other parameters in this simulation are the same as former simulation.

resistance of unit length of the rings measured around the circumference, μ_0 is the relative permeability in vacuum, c_0 is the speed of light in vacuum, and ω is operating angular frequency. a_0, c, g, and r are geometrical parameters given in Fig. 11(a). If the lattice constant is much smaller than the operating wavelength, this medium composed of metamaterial cells can be treated as a continuous medium A, as shown in Fig. 11(b). For regions 2 and 3, we can use metamaterial with closed ring units [26] and ferromagnetic materials [27] to realize the required extremely small permeability (i.e., close to zero) and the permeability larger than 1, respectively.

To verify the effectiveness of our proposal, we numerically studied the performance of our MTP composed of layered isotropic medium, and the magnetic field norm distribution is shown in Fig. 12. In Fig. 12(a), we plot for the case where a point magnetic dipole is chosen as the EM source without our MTP. Fig. 12(b) shows the MTP composed of the layered medium can transfer larger part of source energy to the right side of the MTP, hence our proposal is feasible. Here, the MTP and the inner air region are drawn as diagram to show the implementation method.

As the function of the MTP is to shift any sources inside it by a predesigned distance d away from it, it can not only transfer energy but also information from the sources to a signal receiver far away from it (i.e., the proposed MTP can also be used for wireless communication). If we use many MTPs to shift the sources inside them to the same spatial position (i.e., the images overlap each other), we can also achieve magnetic power collection and concentration.

V. Conclusion

In conclusion, a MTP designed by TO is shown to be capable of greatly enhancing wireless energy transfer efficiency. Compared with a magnetic superlens of the same size, our MTP can give a much better performance (e.g., the enhancement factors A defined by (4) for the magnetic superlens and our MTP are of about two times and two orders, respectively). Three-dimensional numerical simulations have been given to verify the performance of the proposed MTP. Even for the case where loss is considered, our MTP can still give a good performance. Our design points out a new way for improving the energy transfer efficiency in WPT systems, which can be further implemented with metamaterial.

References

[1] N. Tesla, “Apparatus for transmitting electrical energy,” U.S. Patent 1 119 732, Dec. 1, 1914.

[2] F. Zhang *et al.*, “Wireless energy transfer platform for medical sensors and implantable devices,” in *Proc. Annu. Int. Conf. IEEE Eng. Med. Biol. Soc.*, 2009, pp. 1045–1048.

[3] J. Kim *et al.*, “Microwave power transmission using a flexible rectenna for microwave-powered aerial vehicles,” *Smart Mater. Struct.*, vol. 15, no. 5, pp. 889–892, Aug. 2004.

[4] A. Karalis, J. D. Joannopoulos, and M. Soljačić, “Efficient wireless non-radiative mid-range energy transfer,” *Ann. Phys.*, vol. 323, no. 1, pp. 34–48, Jan. 2008.

[5] A. Kurs *et al.*, “Wireless power transfer via strongly coupled magnetic resonances,” *Science*, vol. 317, no. 5834, pp. 83–86, Jul. 2007.

[6] X. Wei, Z. Wang, and H. Dai, “A critical review of wireless power transfer via strongly coupled magnetic resonances,” *Energies*, vol. 7, no. 7, pp. 4316–4341, Jul. 2014.

[7] Y. Urzhumov and D. R. Smith, “Metamaterial-enhanced coupling between magnetic dipoles for efficient wireless power transfer,” *Phys. Rev. B*, vol. 83, no. 20, pp. 99–105, May 2011.

[8] G. Lipworth *et al.*, “Magnetic metamaterial superlens for increased range wireless power transfer,” *Sci. Rep.*, vol. 4, no. 3642, pp. 1–6, Jan. 2014.

[9] A. L. A. K. Ranaweera, T. P. Duong, and J. W. Lee, “Experimental investigation of compact metamaterial for high efficiency mid-range wireless power transfer applications,” *J. Appl. Phys.*, vol. 116, no. 4, pp. 1–8, Jul. 2014.

[10] Y. Zhang, H. Tang, C. Yao, Y. Li, and S. Xiao, “Experiments on adjustable magnetic metamaterials applied in megahertz wireless power transmission,” *AIP Adv.*, vol. 5, no. 1, pp. 2075–2084, Jan. 2015.

[11] J. B. Pendry, D. Schurig, and D. R. Smith, “Controlling electromagnetic fields,” *Science*, vol. 312, no. 5781, pp. 1780–1782, Jun. 2006.

[12] H. Chen, C. T. Chan, and P. Sheng, “Transformation optics and metamaterials,” *Nat. Mater.*, vol. 9, no. 5, pp. 387–396, Apr. 2010.

[13] C. Navau, J. Prat-Camps, and A. Sanchez, “Magnetic energy harvesting and concentration at a distance by transformation optics,” *Phys. Rev. Lett.*, vol. 109, no. 26, pp. 1–5, Dec. 2012.

[14] J. Prat-Camps, C. Navau, and A. Sanchez, “Quasistatic metamaterials: magnetic coupling enhancement by effective space cancellation,” *Adv. Mater.*, vol. 28, pp. 1–6, Apr. 2016.

[15] F. Sun, Y. Liu, and S. He, “True dynamic imaging and image composition by the optical translational projector,” *J. Opt.*, vol. 18, no. 4, pp. 1–7, Apr. 2016.

[16] A. Greenleaf, Y. Kurylev, M. Lassas, and G. Uhlmann, “Electromagnetic wormholes and virtual magnetic monopoles from metamaterials,” *Phys. Rev. Lett.*, vol. 99, no. 18, pp. 1–4. Nov. 2007.

[17] D. Schurig *et al.*, “Metamaterial electromagnetic cloak at microwave frequencies,” *Sci.*, vol. 314, no. 5801, pp. 977–980, Nov. 2006.

[18] X. J. Wei, F. M. Hui, C. Qiang, and T. J. Cui, “Illusion media: Generating virtual objects using realizable metamaterials,” *Appl. Phys. Lett.*, vol. 96, no. 12, pp. 1–3, Mar. 2010.

[19] D. Huang *et al.*, “Magnetic superlens-enhanced inductive coupling for wireless power transfer,” *J. Appl. Phys.*, vol. 111, no. 6, pp. 1–8, Mar. 2012.

[20] S. Y. R. Hui, W. Zhong, and C. K. Lee, “A critical review of recent progress in mid-range wireless power transfer,” *IEEE Trans. Power Electron.*, vol. 29, no. 9, pp. 4500–4511, Mar. 2013.

[21] C. Kurter, T. Lan, L. Sarytchev, and S. M. Anlage, “Tunable negative permeability in a three-dimensional superconducting metamaterial,” *Phys. Rev. App.*, vol. 3, no. 5, pp. 1–6, May 2015.

[22] Y. J. Huang, G. J. Wen, T. Q. Li, and K. Xie, “Low-loss, broadband and tunable negative refractive index metamaterial,” *J. Electromagn. Anal. Appl.*, vol. 2, no. 2, pp. 104–110, Feb. 2010.

[23] F. Sun and S. He, “Extending the scanning angle of a phased array antenna by using a null-space medium,” *Sci.Rep.*, vol. 4, no. 6832, pp. 1–6, Oct. 2014.

[24] J. D. Baena, R. Marqués, F. Medina, and J. Martel, “Artificial magnetic metamaterial design by using spiral resonators,” *Phys. Rev. B*, vol. 69, no. 014402, pp. 1–5, Jan. 2004.
[25] J. B. Pendry, A. J. Holden, D. J. Robbins, and W. J. Stewart, “Magnetism from conductors and enhanced nonlinear phenomena,” *IEEE Trans. Microw. Theory Tech.*, vol. 47, no. 11, pp. 2075–2084, Nov. 1999.
[26] H. Chen, L. Huang, X. Cheng, and H. Wang, “Magnetic properties of metamaterial composed of closed rings,” *Prog. Electromagn. Res.*, vol. 115, pp. 317–326, Apr. 2011.
[27] T. T. Srinivasan, P. Ravindranathan, L. E. Cross, R. Roy, and R. E. Newnham, “Studies on high-density nickel zinc ferrite and its magnetic properties using novel hydrazine precursors,” *J. Appl. Phys.*, vol. 63, no. 8, pp. 3789–3791, Apr. 1988.

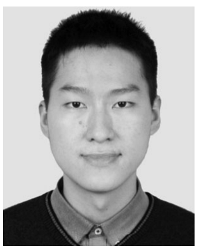

Shichao Li was born in Chongqing, China, in 1995. He received the B.E. degree in opto-electronics science and engineering from Zhejiang University, Hangzhou, China, in 2017, he will start working toward the Ph.D. degree in computer science and engineering from Hong Kong University of Science and Technology, Hong Kong, in the same year.

From 2014 to 2016, he was a Research Assistant in the Center for Optical and Electromagnetic Research, Zhejiang University. His research interests include device modeling and simulation, image processing, and computational methods.

Mr. Li received the China National Scholarship in 2014 and Hong Kong Ph.D. Fellowship Scheme in 2017.

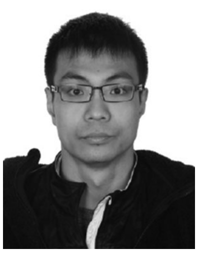

Fei Sun received the Ph.D. degree in electric engineering from the Royal Institute of Technology, Stockholm, Sweden, in 2014, and in optical engineering from Zhejiang University, Hangzhou, China in 2015, where he is currently a Postdoctor in the College of Optical Science and Engineering.

His current research interests include transformation optics, novel optical devices, electromagnetic metamaterials and acoustic devices. He has first authored 21 papers in refereed international journals.

Di An received the B.E. degree in opto-electronics science and engineering from Zhejiang University, Hangzhou, China, in 2017, and he will work toward the master’s degree in electrical engineering in Northwestern University, Evanston, IL, USA, in the same year.

He is currently a Senior Student majoring in opto-electronics science and engineering in Zhejiang University, China. His research interests include optical coherence tomography, machine learning and computer vision.

Sailing He (M’92–SM’98–F’13) received the Licentiate of Technology and the Ph.D. degree in electromagnetic theory from the Royal Institute of Technology (KTH), Stockholm, Sweden, in 1991 and 1992, respectively.

Since then, he has been in the same division of the Royal Institute of Technology as an Assistant Professor, an Associate Professor, and a Full Professor. He also serves as the Director for a joint research center between KTH and Zhejiang University, Hangzhou, China. His current research interests include applied electromagnetics, electromagnetic metamaterials, optoelectronics, microwave photonics, and biomedical applications. He has first authored one monograph (Oxford University Press) and authored/c-authored about 500 papers in refereed international journals.

Dr. He has given many invited/plenary talks in international conferences, and has served in the leadership for many international conferences.